Influence of twin-screw processing conditions on structure and properties of polypropylene - organoclay nanocomposites

Trystan Domenech, Edith Peuvrel-Disdier, Bruno Vergnes

Influence of Twin-Screw Processing Conditions on Structure and Properties of Polypropylene - Organoclay Nanocomposites

T. Domenech*, E. Peuvrel-Disdier, B. Vergnes

MINES ParisTech, Centre de Mise en Forme des Matériaux, UMR CNRS 7635
BP 207, 06904 Sophia Antipolis (France)

**Corresponding author: trystan.domenech@mines-paristech.fr*

Abstract. Melt processing is a commonly used method for producing polymer based nanocomposites. Addition of nanofiller such as organomodified montmorillonite layered clay (OMMT) is mostly used to enhance tensile, impact and barrier properties of the neat matrix. Initial clay agglomerates need to be finely dispersed within the matrix during the process in order to form exfoliated nanostructures. Interactions between non polar thermoplastics such as polyolefins and organomodified clay are usually promoted by the presence of a compatibilizer. Maleic anhydride grafted polypropylene (PP-g-MA) is generally used in the case of polypropylene matrix (PP). Besides the need to use a compatibilizer, a good state of dispersion and distribution of the clay requires optimized processing conditions.
Many studies have focused on the influence of nanocomposite formulations on their final properties, but few have paid attention to the nanostructure sensitivity to processing conditions. This study deals with the influence of extrusion parameters such as screw speed, feed rate and barrel temperature on the nanocomposite structure and its consequences on final properties. Nanocomposites of polypropylene, maleated polypropylene and organomodified montmorillonite with respective mass fraction of 85/10/5 were prepared with a co-rotating twin-screw extruder using a masterbatch dilution method. The structure of obtained nanocomposites was quantified by scanning and transmission electron microscopy (SEM, TEM), X-ray diffraction and dynamic rheometry.

Introduction

Polymer/layered silicate nanocomposites materials have triggered huge interest from both academic and industrial point of view since their properties and potential applications have been highlighted by Toyota researchers in the early 90's [1]. Indeed, these materials revealed improvement in mechanical and gas barrier properties, fire retardant behaviour and dimensional stability compared to the neat polymer matrix [2-4]. Furthermore, observed properties improvement generally occurs at low filler concentration (between 1 and 10 wt%) and is believed to be linked to the fine structure of dispersed/distributed clay layers within the polymer matrix, featuring high aspect ratio and specific surface of the organic filler. Formation of such hybrid materials can either be achieved by in situ polymerization or melt mixing process, melt mixing being more adapted to industrial scale production for cost and processability reasons. In the case of polyolefin matrix like polypropylene, low affinity between non-polar polymer chains and polar silicate surface is an obstacle to the formation of exfoliated structure, as opposed to polymer containing polar functions like polyamide. Addition of a compatibilizer like polypropylene grafted with maleic anhydride and treatment of the layered silicate by organic surfactant has shown promising ability to overcome this affinity issue [4-6]. Nevertheless, reaching a good state of dispersion for these systems remains difficult and requires optimal processing conditions. Surprisingly, only a few studies about the impact of processing conditions on nanocomposites' structure can be found in the literature [2, 6-11]. In this paper, we propose to investigate how the processing parameters of twin screw extrusion are related to the final structure of PP/PP-g-MA/OMMT nanocomposites.

Materials and experimental methods

Materials. Injection grade isotactic PP homo-polymer (Moplen HP400R) was purchased from Basell Polyolefins. This grade has a 25 g/10 min melt flow index and a density of 0.905 g/cm^3. Its molecular weight distribution was determined by steric exclusion chromatography, giving number average molecular mass M_n = 58500 g/mol and polydispersity index I_p = 3.5. Montmorillonite based organoclay (Dellite 67G) was kindly

supplied by Laviosa Chimica Mineraria (Livorno, Italy). This grade of clay features dimethyl-dehydrogenated-tallow quaternary ammonium as organic modifier with 48 wt% of organic modifier content and CEC (cation exchange capacity) of 115 meq/100g. Specific weight of the organoclay powder is 1.7 g/cm^3. Polypropylene grafted with maleic anhydride (Eastman G-3015) was purchased from Eastman and used as a compatibilizer. This PP-g-MA grade has a MA content of 3.1 wt% and a density of 0.913 g/cm^3. Its number average molecular mass M_n is 24800 g/mol and its polydispersity index I_p is 1.9.

Composite preparation. Nanocomposites were prepared by twin screw extrusion using a masterbatch dilution method. The masterbatch was compounded by the Danish Technological Institute. It contains 40 wt% of PP, 40 wt% of PP-g-MA and 20 wt% of organoclay, i.e. a compatibilizer to organoclay ratio of 2:1.
The second step of the preparation consisted in diluting the masterbatch into polypropylene in order to obtain a final PP/PP-g-MA/OMMT formulation of 85/10/5 wt%. This processing step was achieved on a Rheomex PTW24 corotating twin screw extruder (ThermoFisher, Massachusetts, USA). This laboratory scale extruder (D = 24 mm, L/D = 40) features the screw profile shown in Fig. 1. Material is fed by a DDW-MD3-DDSR20-10 gravimetric feeder (Brabender, Duisburg, Germany). Extruded strands were cooled through a waterbath and pelletised using a Thermo Fisher PRISM Varicut pelletiser.

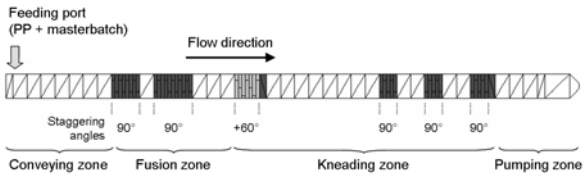

Fig. 1. Screw profile representation

Processing parameters were varied in terms of screw speed N and feed rate Q. A first set of trials was performed with constant barrel temperature T_b = 180°C and feed rate Q = 3 kg/h for several screw speeds of 100, 300, 500, 700 and 900 rpm. Influence of the feed rate was also investigated, running the extruder with constant barrel temperature (T_b = 180°C) and screw speed (N = 500 rpm) for various Q values of 3, 6, 10, 15 and 20 kg/h. For each processing condition, melt temperature at the die exit was measured by introducing a thermocouple into the bulk of the extruded material. Minimum residence time t_{min} was also evaluated by adding one pellet of coloured material into the extruder. Screw torque C was recorded during extrusion, enabling the calculation of specific mechanical energy (SME):

$$SME = \frac{\alpha \cdot C \cdot N}{Q} \qquad (1)$$

where α depends on motor power, maximum screw speed and maximum torque.

Morphology characterization. Dispersion of layered silicate within polymer matrix via melt mixing can lead to a wide size distribution of the clay filler, from nanoscale exfoliated single platelets to microscale clay agglomerates. A systematic characterization of organoclay dispersion was performed on both microscopic and nanoscopic scale, depending on processing conditions. Agglomerate size distributions were determined by scanning electron microscopy (SEM), using a Philips XL30 with accelerating voltage of 15 kV. Back-scattered electron detector was used to obtain phase contrast between clay filler and polymer matrix. Prior to SEM observations, sample surfaces were polished to obtain flat surfaces with roughness parameter R_a close to 1 µm and then sputter coated with Au/Pd target (deposit thickness around 10 nm). Quantitative size characterisation of clay agglomerates was obtained using Visilog 5.0 software. Each area occupied by clay agglomerates on the observed surfaces was calculated from the SEM pictures. Microscale clay dispersion was then quantified by the parameter A_r, which is the ratio between the total area filled by clay agglomerates and the analysed area A_0:

$$A_r = \frac{\sum A_{clay}}{A_0} \qquad (2)$$

Clay agglomerates with equivalent diameter inferior to 10 µm were not taken into account. Analysed surface A_0 was 17.2 mm^2.
High magnification observations were done using transmission electron microscopy (TEM). Observations were performed with a Philips CM12 operating at 120 kV acceleration tension using a LaB_6 cathode. Ultra-thin sections were prepared from the central zone of an injection moulded tensile bar (in the plan normal to the flow direction) using Ultracut ultracryomicrotome (Leica Microsystems, Wetzlar, Germany) equipped with Cryotrim and 2 mm Cryo diamond knives (Diatome, Biel, Switzerland). Glass transition temperature of both PP and PP-g-MA being around -10°C, ultra-thin sections were cut at

-100°C with a thickness of 50 nm and then collected on a copper grid.

X-Ray Diffraction analysis. Layered structure of montmorillonite gives rise to X-ray diffraction peaks corresponding to its interplanar distances, particularly the basal spacing d_{001} which is the addition of one single platelet thickness (0.96 nm) with the interlayer distance. Intercalation of polymer chains between the clay galleries leads to an increased basal spacing [12, 13]. As a consequence, X-ray diffraction is often used to estimate the level of intercalation. Nanocomposites corresponding to each processing conditions were scanned using Philips Xpert' Pro X-ray diffractometer with Cu K_α radiation (λ = 1.5405 Å). The original organoclay powder was also analysed.

Rheological analysis. Small amplitude oscillatory shear measurements were performed on an Advanced Rheometric Expansion System (ARES) controlled strain rheometer (TA Instruments, Delaware, USA). Parallel plate geometry with a 25 mm diameter and a 1 mm gap was used. All rheological tests were conducted in the melt state with a fixed temperature of 180°C under nitrogen environment. For each processing condition, a strain amplitude sweep was run up to 300 % at a constant angular frequency of 1 rad/s to determine the linear viscoelastic domain. Both time and frequency sweep tests were then launched at a fixed strain within the linear viscoelastic range, following a procedure described in the further section. All rheological measurements were performed on disc-shaped samples prepared by compression molding using a Carver M 3853-0 hot press (Carver, Indiana, USA) at 180°C under 25 MPa pressure for 8 min. Aluminium circular frame with 25 mm diameter and 1.5 mm thickness was used as a mould. A new sample was used for each rheological test.

Results and discussion

Morphology of organoclay based nanocomposites. Organomodified layered silicates have a wide size range. The smallest montmorillonite particle corresponds to an individualised platelet with approximately 1 nm thickness and a few hundreds nm in lateral dimensions. These platelets are naturally present under the form of stacks containing a few tens of sheets, commonly referred as tactoids. Organoclays are generally available as powder composed of agglomerates with characteristic size superior to 10 µm (Fig. 2). Agglomerates are themselves composed of aggregated tactoids. Incorporation of organoclay into a melt polymer matrix during melt mixing process, such as twin screw extrusion, will first lead to powder grain agglomeration that will then be broken down along the screw profile, the dispersion efficiency being related to the processing conditions.

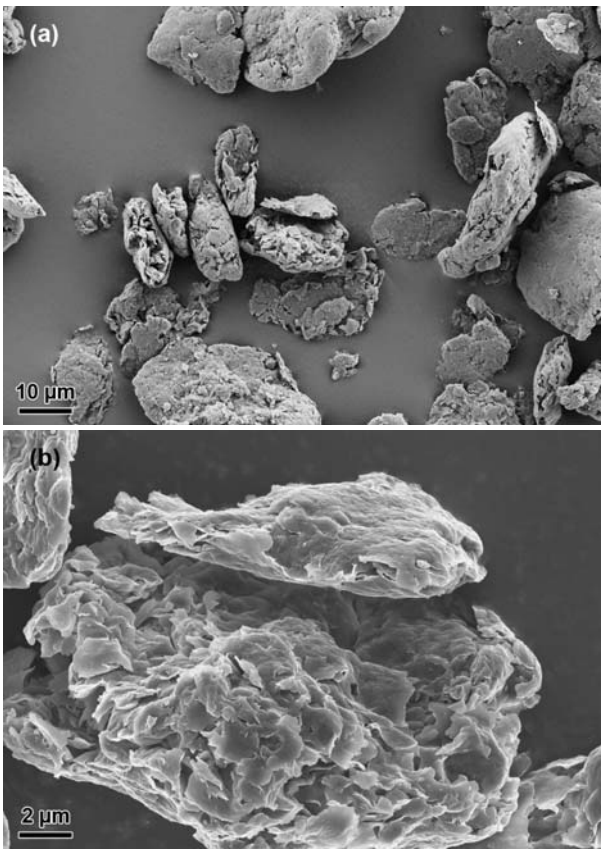

Fig. 2. SEM micrographs of Dellite 67G powder captured with secondary electron detector at different magnifications, (a) x1000, (b) x5000

Influence of screw speed on nanocomposite structure. Dispersion of agglomerates during extrusion depends on the shear stress intensity thus on screw speed. The dependence of clay agglomerate morphology with *N* is represented in Fig. 4. Black zones are clay and grey background is the PP/PP-g-MA matrix. These pictures reveal the presence of agglomerates with equivalent diameter comprised between 10 and 180 µm, depending on screw speed. It can be noted that the original organoclay powder agglomerate size is within the 10 to 40 µm range as shown in Fig.2, which means that agglomeration of the powder occurred during the production of the masterbatch due to its high concentration in organoclay (20 wt%). However, it is clear that increasing *N* leads to a significant reduction of the biggest agglomerate size. The number of agglomerates per surface unit, referred to as the agglomerate surface

density, is also a good indicator of microscale dispersion. Fig. 3 shows that both area ratio and agglomerate surface density drastically decrease when screw speed is increased.

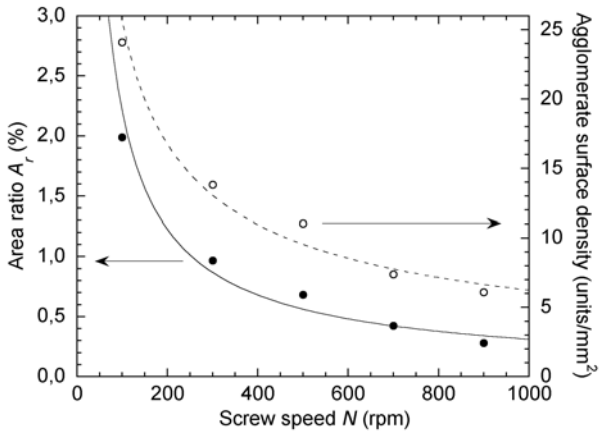

Fig. 3. Dependence of area ratio and agglomerate surface density with screw speed.

Higher magnification micrographs obtained by TEM are presented on Fig. 5. The presence of clay tactoids and exfoliated sheets can be observed. Transition from 100 to 500 rpm reveals a decrease in tactoids thickness (from 100 to 20 nm in average), leading to reduced distances between clay particles. On the other hand, the increase in screw speed from 500 to 900 rpm did not cause clear variations of the nanostructure.

XRD analysis showed that diffraction peaks related to the basal spacing of the clay remain whatever the used screw speed. This means that the exfoliation is only partial, which was already clear from SEM and TEM observations. A slight increase in basal spacing was observed for the nanocomposite processed at 100 rpm compared to the Dellite 67G powder (from 3.45 to 3.60 nm) indicating a possible intercalation. Higher screw speed values led to a small decrease in basal spacing that can be due to the degradation of the organoclay interlayer surfactant which is known to provoke interlayer spacing reduction. This possible surfactant degradation could be linked to the increase in melt temperature which is induced by the increase of viscous dissipation with screw speed.

Rheological behaviour of the nanocomposites in the melt state is sensitive to the nanostructure, especially in the linear viscoelastic domain. As processing conditions play an important role on the nanocomposite structure, it is important to determine the linear domain for each processing conditions. Fig. 6 shows the results of dynamic strain sweep tests performed on the nanocomposites processed for various screw speeds, as well as on the binary mix of PP/PP-g-MA (denoted *matrix*) with the same proportions as for the samples containing organoclay. Important reduction of the linear domain is observed for the nanocomposites compared to the matrix. It can also be noted that the reinforcement effect of the clay, resulting in an increase of the plateau modulus as well as a decrease in linear domain, is more pronounced when the screw speed is increased.

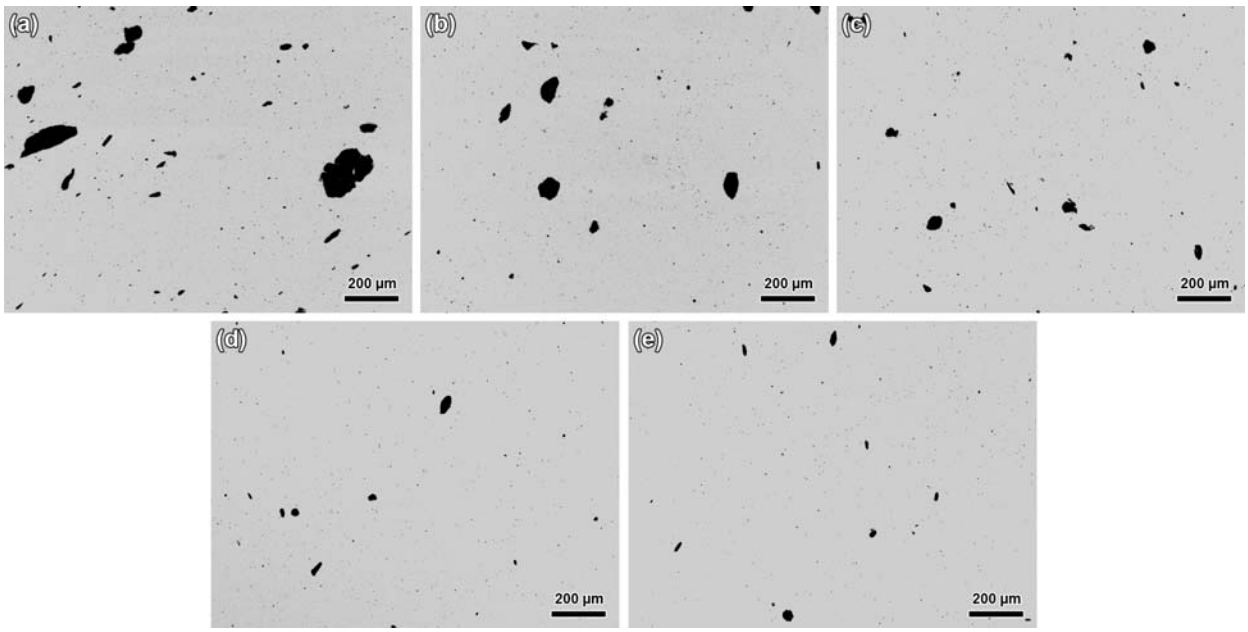

Fig. 4. SEM micrographs (x200) of clay agglomerates within PP/PP-g-MA matrix at fixed T_b (180°C) and Q (3 kg/h) for various N values (a) 100 rpm (b) 300 rpm (c) 500 rpm (d) 700 rpm (e) 900 rpm

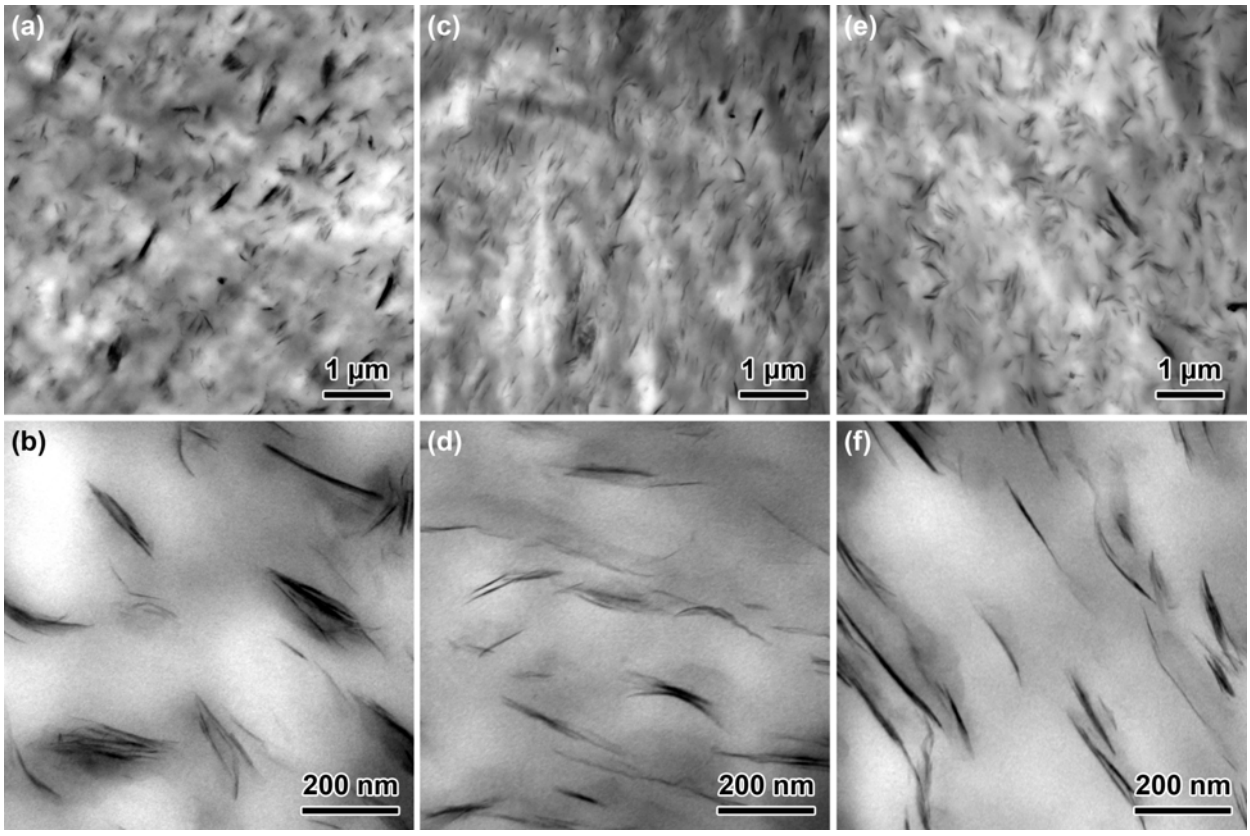

Fig. 5. Bright field TEM micrographs at x11500 and x88000 magnifications. Nanocomposites are processed at fixed T_b (180°C) and Q (3 kg/h) for various N values: (a,b) 100 rpm (c,d) 500 rpm (e,f) 900 rpm

We assume that this observation is linked to the improvement of the dispersion state obtained by the increase of N, inasmuch as it was noticed by SEM and TEM morphological characterization.

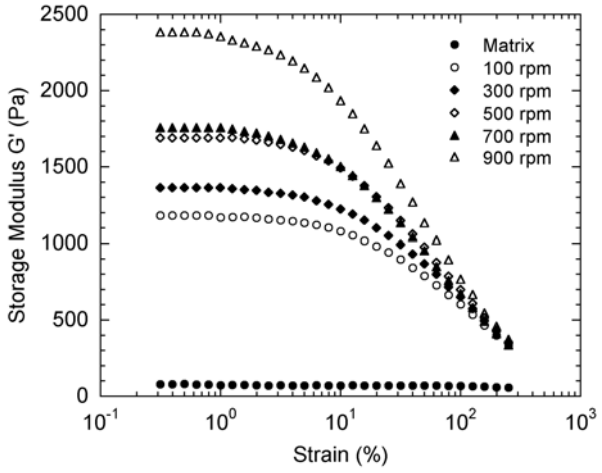

Fig. 6. Storage modulus as a function of strain at fixed angular frequency (ω = 1 rad/s). Nanocomposites are processed at fixed T_b (180°C) and Q (3 kg/h)

As a consequence, all rheological tests were performed with a fixed strain of 1% in order to be within the linear viscoelastic domain. It is also important to check the evolution of the rheological parameters with time. Dynamic time sweep test results for a period of 7200 seconds are plotted on Fig. 7. Unlike the matrix whose storage modulus is almost constant over this period of time, nanocomposites exhibit a continuous increase of their storage modulus along with time. It can be noted that a higher screw speed results in a higher storage modulus over the whole time range.

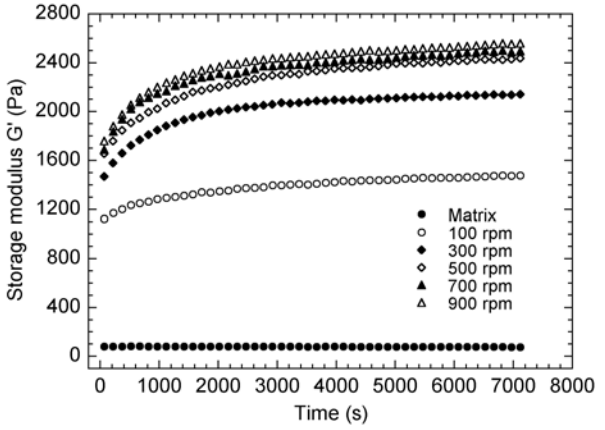

Fig. 7. Storage modulus as a function of time at fixed angular frequency ω=1 rad/s. Nanocomposites processed at fixed T_b (180°C) and Q (3 kg/h)

The increase in storage modulus is also more pronounced during the first 2000 seconds than during the rest of the test, where the increase is

slowed down but still going on. The same behaviour is observed on the loss modulus *G*" although it is much less pronounced. This phenomenon has been observed for clay suspension materials [14-16] as well as for other polymer based layered silicate nanocomposites [17-20]. This particular behaviour is believed to reflect the evolution of clay-clay interactions due to the motion/disorientation of anisotropic fine clay particles [21]. However, in order to perform consistent rheological measurements, each nanocomposite sample is kept under quiescent conditions within the rheometer at 180°C for 1800 seconds prior to frequency sweep tests, in order to "stabilize" the rheological behaviour of the material (this protocol has previously been used by some authors [6, 7, 22]). Results of the frequency sweep tests are plotted in Fig. 8. Addition of clay into the polymer matrix leads to a transition from a liquid-like behaviour (matrix) to a solid-like behaviour (nanocomposites) in the terminal zone (low frequencies), with the onset of a *G'* plateau and an increase in complex viscosity as the frequency decreases. Such rheological behaviour is assumed to be the response of a percolation network formed by finely dispersed clay tactoids and exfoliated sheets [22, 23]. A model based on a Carreau-Yasuda law with the addition of a yield stress term perfectly describes the complex viscosity dependence with the frequency [24]:

$$\eta^*(\omega) = \frac{\sigma_0}{\omega} + \eta_0\left[1+(\lambda\omega)^a\right]^{\frac{n-1}{a}} \qquad (3)$$

Rheological data were fitted using this model. Fig. 8b shows both data (symbols) and fit using Eq. (3) (solid lines). Increasing the extent of exfoliation leads to higher *G'* plateau and complex viscosity values at low frequencies (under 1 rad/s) due to stronger clay interactions, which also leads to higher values in melt yield stress σ_0. It is thus possible to use σ_0 as a quantitative parameter of the exfoliation level. The PP/PP-g-MA matrix has a classical Carreau-Yasuda behaviour with a Newtonian plateau in the terminal zone (Fig. 8b) with a zero melt yield stress. On the other hand, σ_0 for nanocomposites depend on the screw speed as it can be seen in Fig. 8c. Up to N = 500 rpm, σ_0 increases linearly with N and then saturates to a limit at higher screw speeds. It would mean that the increase in screw speed no longer contributes to the exfoliation of the organoclay above a certain point. TEM micrographs shown in Fig. 5 also suggest, in a more qualitative way, that the

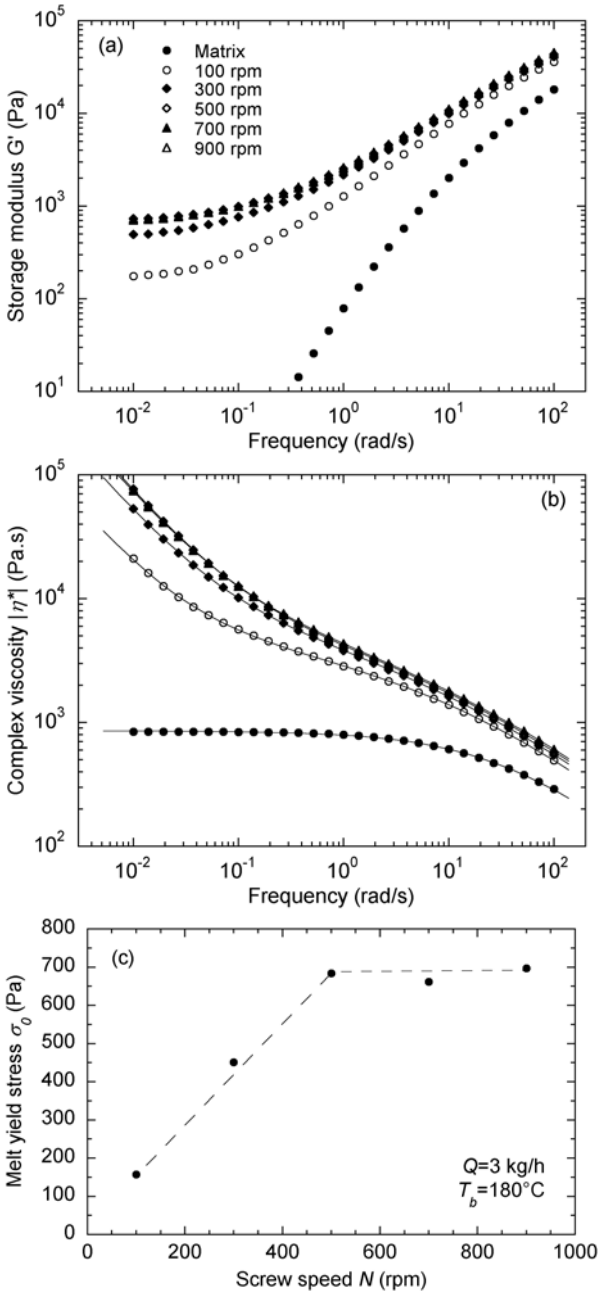

Fig. 8. Frequency sweep analysis: (a) storage modulus versus frequency (b) complex viscosity versus frequency (c) melt yield stress dependence with screw speed. Nanocomposites are processed at fixed T_b (180°C) and Q (3 kg/h)

nanostructure does not change much above N = 500 rpm.

Influence of feed rate on nanocomposite structure. Even though screw configuration or screw speed can affect the residence time distribution, it is generally much more sensitive to feed rate value [25]. As possible erosion of the clay sheets would be sensitive to the residence time, it is important to look at the impact of feed rate on the final nanocomposites structure. SEM

observations are represented in Fig. 10 whereas quantitative analysis results are plotted in Fig. 9.

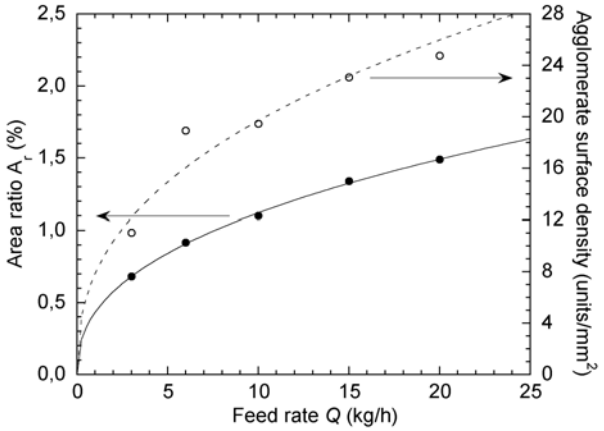

Fig. 9. Dependence of area ratio and agglomerate surface density with feed rate.

When feed rate is increased, thus when residence time is decreased, it is quite obvious that the dispersion quality of the organoclay is reduced, leading to the presence of bigger organoclay agglomerates and also to a higher number of agglomerates. The same remark can be done about the aggregates, considering TEM acquisitions presented in Fig. 12. The thickness of the clay tactoids also increases when feed rate is increased. The minimum residence times t_{min} were measured as 130, 42, 31, 24 and 20 seconds for 3, 6, 10, 15 and 20 kg/h in feed rate, respectively. This clearly shows that the state of dispersion is sensitive to extrusion residence time. Such morphological variations should also affect the rheological response of the nanocomposites. Results of the dynamic frequency sweep tests are plotted in Fig. 11a.

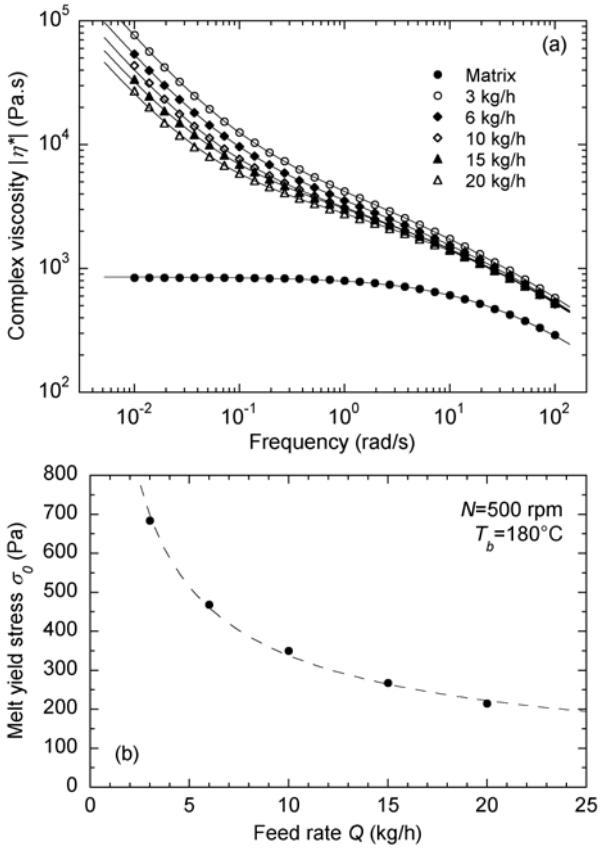

Fig. 11. Frequency sweeps analysis: (a) complex viscosity versus frequency (b) melt yield stress dependence with feed rate.

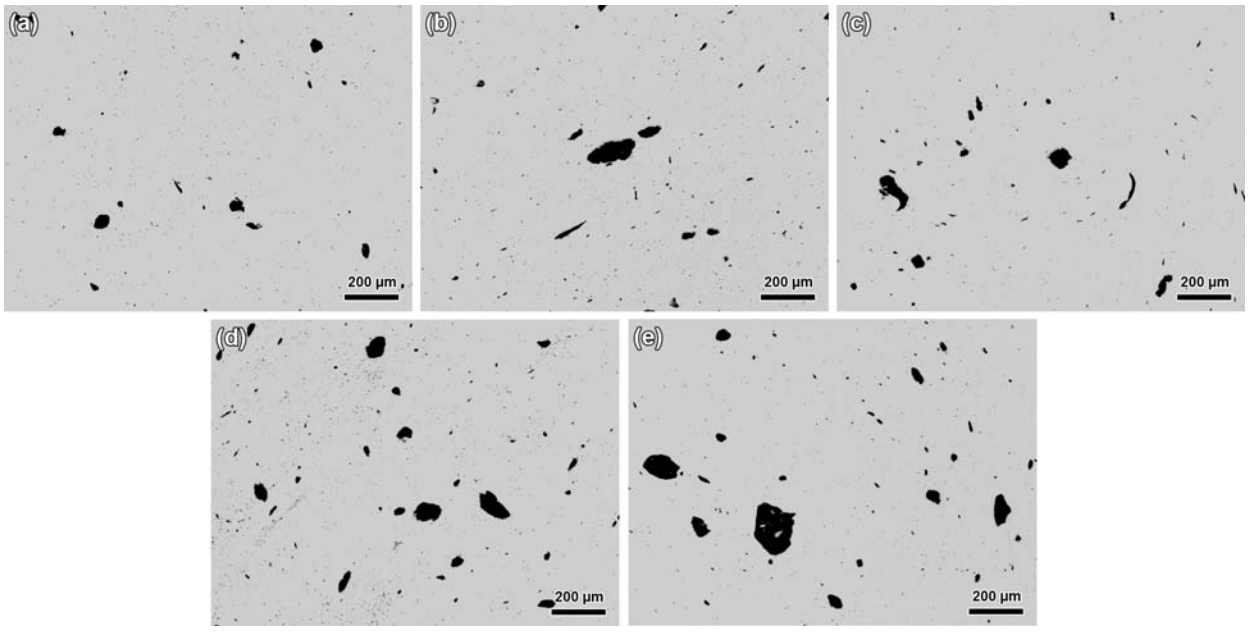

Fig. 10. SEM micrographs (x200) of clay agglomerates within PP/PP-g-MA matrix at fixed T_b (180°C) and N (500 rpm) for various Q values (a) 3 kg/h (b) 6 kg/h (c) 10 kg/h (d) 15 kg/h (e) 20 kg/h

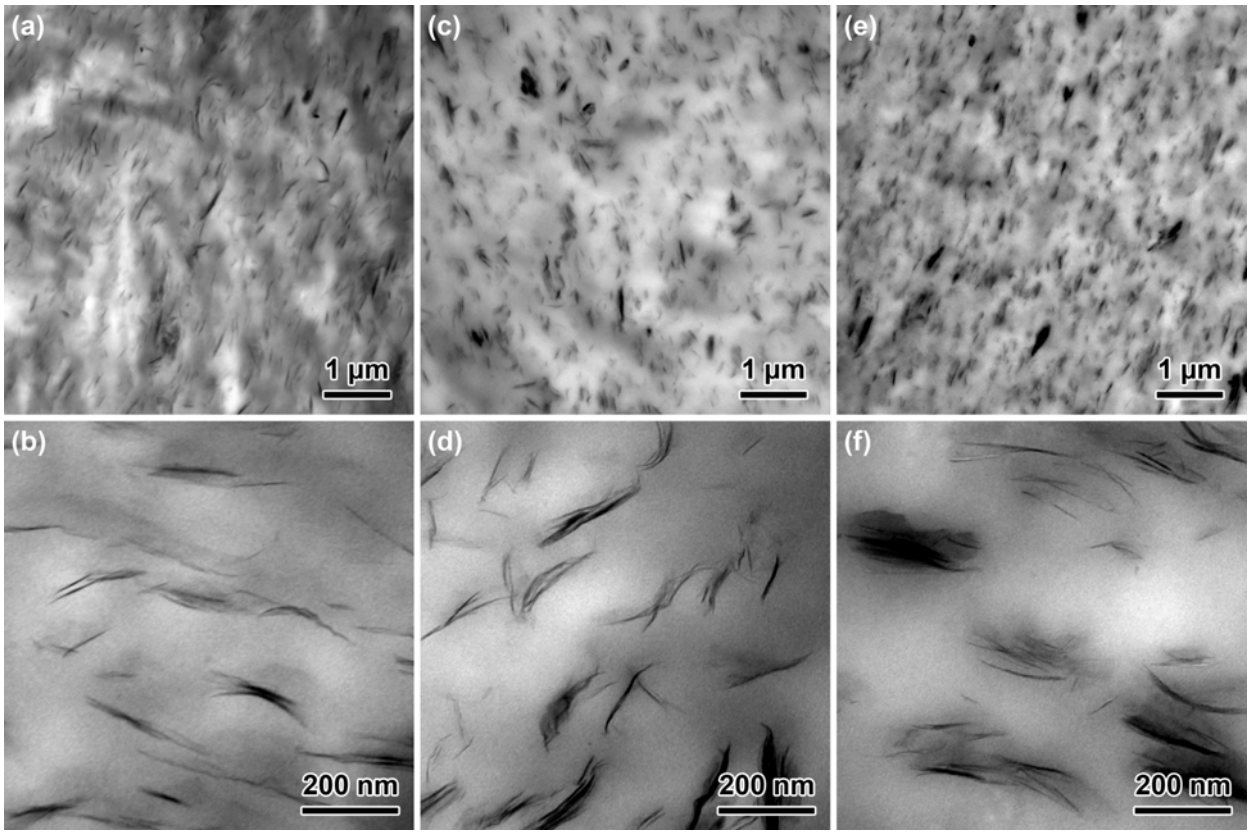

Fig. 12. Bright field TEM micrographs at x11500 and x88000 magnifications. Nanocomposites are processed at fixed T_b (180°C) and N (500 rpm) for various Q values: (a,b) 3 kg/h (c,d) 10 kg/h (e,f) 20 kg/h

Again, the rheological behaviour of the nanocomposites differs from that of the PP/PP-g-MA matrix, especially at low frequencies. Solid lines in Fig. 11a represent the fit obtained from experimental data (symbols) using Eq. (3). Melt yield stress values are plotted as a function of feed rate in Fig. 11b, exhibiting a decreasing dependency of power law type. The exfoliation level is therefore favoured by lower values of feed rate, which is consistent with the observations performed by TEM. At both microstructure and nanostructure level, the dispersion quality of the organoclay within the PP/PP-g-MA matrix seems to be optimal for low feed rate values which means high residence times. This statement might be related to the kinetics of the dispersion process of organomodified montmorillonite within polymer matrix, where diffusion of polymer chains within the clay galleries and erosion of clay sheets from the surface of agglomerates are often evoked in the literature [9, 12, 13]. Similar trends of the melt yield stress dependence with mixing time were obtained by Lertwimolnun and Vergnes [6] using an internal mixer where the mixing time can easily be controlled.

Overall influence of processing conditions on nanocomposite structure. We have seen that both screw speed and feed rate have an important impact on the final structure of the nanocomposites. The quality of dispersion is improved by increasing shear intensity and residence time. These statements were based on microscale and nanoscale quantitative analysis using SEM and dynamic rheometry, as well as qualitative interpretation of TEM observations. Nevertheless, the optimisation of processing parameters would be facilitated if the structure of the nanocomposites could be linked to a unique parameter. The specific mechanical energy (*SME*), introduced in section 2.2, quantifies the level of energy which is transferred to the material by mechanical input during extrusion. It takes both screw speed and feed rate values into account (see Eq. (1)). Area ratio and melt yield stress are plotted as a function of *SME* in Fig. 13 for all the processing conditions used (screw speed and feed rate variations). The first important point to notice is that mastercurves are obtained for both A_r and σ_0, which means that *SME* can be considered as a key parameter of the state of dispersion for the obtained nanocomposites. It is found that the area ratio decreases with the *SME* following a power law dependence. Similar relationship has been recently found by Villmow et al. [26] in the case

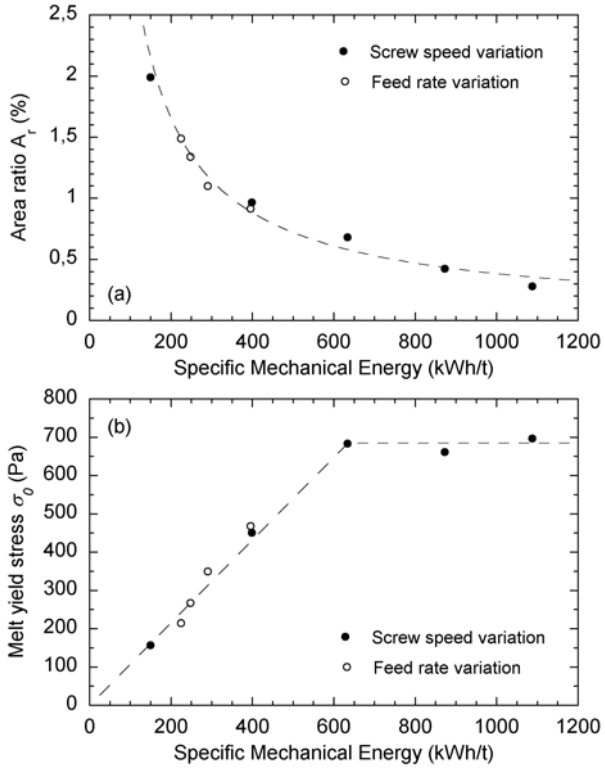

Fig. 13. Mastercurves obtained for screw speed and feed rate variations (a) A_r as a function of *SME* (b) σ_0 as a function of *SME*

of polycaprolactone/multi wall carbone nanotubes nanocomposites obtained by twin screw extrusion process. Relationships between melt yield stress and *SME* were also shown by Lertwimolnun and Vergnes [8]. As already mentioned in section 3.2, the melt yield stress grows linearly with *SME* until a value close to 600 kWh/t. Above that critical *SME* value, σ_0 stabilizes at a plateau value, meaning that no more exfoliation seems to occur. Médéric et al. [11] found a similar behaviour in the case of polyamide-12/organoclay processed in an internal mixer, although the critical *SME* value was found to be much lower (around 140 kWh/t) which means that this parameter might depend on the polymer-clay affinity. Literature agrees that dispersion of organoclay into polymer matrix by melt mixing is usually easier in the case of polyamide comparatively to polyolefin, which could explain why a lower optimal *SME* is found in the case of polyamide matrix.

Conclusions

PP/PP-g-MA/OMMT nanocomposites with 5 wt% of organoclay concentration and a fixed PP-g-MA/organoclay ratio of 2:1 were prepared by twin screw extrusion using a masterbatch dilution method. The influence of processing conditions on the nanocomposite structure has been investigated over a wide range of screw speeds and feed rates. Morphological characterization of the samples was performed using SEM and TEM. Melt rheological analyses in the linear viscoelastic domain were carried out and the quality of organoclay dispersion within the PP/PP-g-MA matrix has been quantitatively characterized. Both screw speed and feed rate were found to have an important effect on the nanocomposite structure. These effects can be seen as an influence of the shear intensity and residence time on the dispersion mechanism during extrusion. X-ray diffraction scans showed that characteristic peaks of the layered structure of the clay were still present whatever the condition, meaning that unexfoliated parts of the clay remain into the polymer matrix, which was confirmed by SEM and TEM observations. It also revealed that intercalation occurred during extrusion even though the role of processing conditions on the intercalation process is not important. The impact of screw speed and feed rate on the nanocomposite structure has been described by a unique processing parameter, the specific mechanical energy. Microscale dispersion gets more effective when SME is increased. On the other hand, exfoliation is clearly promoted by the augmentation of SME until a critical value and then levels off, whereas microscale dispersion is still going on. Structuration of nanocomposites using twin screw extrusion can be optimised by working under high SME conditions until a critical limit beyond which exfoliation can no longer be enhanced by the processing conditions.

Acknowledgements

Authors thank Stephanie Bonny, Thierry Colin, Walid Bahloul, Nathalie Bozzolo and Gabriel Monge (CEMEF) for their precious contribution to this work, as well as Aleksey Drozdov (DTI) for gently providing the masterbatch. Financial support by the European Commission through project Nanotough-213436 is gratefully acknowledged.

References

[1] A. Usuki, Y. Kojima, M. Kawasumi, A. Okada, Y. Fukushima, T. Kurauchi, O. Kamigaito, J. Mater. Res., 8, 1179 (1993).
[2] J.W. Cho, D.R. Paul, Polymer, 42, 1083 (2001).
[3] E.P. Giannelis, Adv. Mater., 8, 29 (1996).
[4] D.H. Kim, P.D. Fasulo, W.R. Rodgers, D.R. Paul, Polymer, 48, 5308 (2007).

[5] M. Kato, A. Usuki, A. Okada, J. Appl. Polym. Sci., 66, 1781 (1997).
[6] W. Lertwimolnun, B. Vergnes, Polymer, 46, 3462 (2005).
[7] W. Lertwimolnun, B. Vergnes, Polym. Eng. Sci., 46, 314 (2006).
[8] W. Lertwimolnun, B. Vergnes, Polym. Eng. Sci., 47, 2100 (2007).
[9] H.R. Dennis, D.L. Hunter, D. Chang, S. Kim, J.L. White, J.W. Cho, D.R. Paul, Polymer, 42, 9513 (2001).
[10] R.K. Shah, D.R. Paul, Polymer, 45, 2991 (2004).
[11] P. Médéric, T. Aubry, T. Razafinimaro, Intern. Polym. Proc., 3, 261 (2009).
[12] R. A. Vaia, H. Ishii, E.P. Giannelis, Chem. Mater., 5, 1694 (1993).
[13] R.A. Vaia, K.D. Jandt, E.J. Kramer, E.P. Giannelis, Macromol., 28, 8080 (1995).
[14] C. Mobuchon, P.J. Carreau, M.C. Heuzey, Rheol. Acta, 46, 1045 (2007).
[15] F. Pignon, A. Magnin, J.M. Piau, J. Rheol., 42, 1349 (1998).
[16] E.A. Toorman, Rheol. Acta, 36, 56 (1997).
[17] G. Galgali, C. Ramesh, A. Lele, Macromol., 34, 852 (2001).
[18] J. Li, C. Zhou, G. Wang, D. Zhao, J. Appl. Polym. Sci., 89, 318 (2003).
[19] J. Ren, B.F. Casanueva, C.A. Mitchell, R. Krishnamoorti, Macromol., 36, 4188 (2003).
[20] R. Zouari, T. Domenech, B. Vergnes, E. Peuvrel-Disdier, submitted to J. Rheol. (2011).
[21] M.A. Treece, J.P. Oberhauser, Macromol., 40, 571 (2007).
[22] M.J. Solomon, A.S. Almusallam, K.F. Seefeldt, A. Somwangthanaroj, P. Varadan, Macromol., 34, 1864 (2001).
[23] R. Krishnamoorti, K. Yurekli, Curr. Opin. Colloid Interf. Sci., 6, 464 (2001).
[24] B. Vergnes, Intern. Polym. Proc., in press (2011).
[25] A. Poulesquen, B. Vergnes, Polym. Eng. Sci., 43, 1841 (2003).
[26] T. Villmow, B. Kretzschmar, P. Pötschke, Compos. Sci. Technol., 70, 2045 (2010).